ISSN 1672-9145 **Acta Biochimica et Biophysica Sinica** 2005, **37**(8): 515–524 **CN** 31-1940/Q

A Lipidomic Study of the Effects of *N*-methyl-*N'*-nitro-*N*-nitrosoguanidine on Sphingomyelin Metabolism

Yun HUANG[&#], Jing SHEN[#], Ting WANG, Yan-Ke YU, Fanqing F. CHEN[1], and Jun YANG*

Department of Pathology and Pathophysiology, Center for Environmental Genomics, Zhejiang University School of Medicine, Hangzhou 310031, China;
[1] Molecular Biology Branch, Life Science Division, Lawrence Berkeley National Laboratory, University of California at Berkeley, Berkeley, CA 94720, USA

Abstract Systems biology is a new and rapidly developing research area in which, by quantitatively describing the interaction among all the individual components of a cell, a systems-level understanding of a biological response can be achieved. Therefore, it requires high-throughput measurement technologies for biological molecules, such as genomic and proteomic approaches for DNA/RNA and protein, respectively. Recently, a new concept, lipidomics, which utilizes the mass spectrometry (MS) method for lipid analysis, has been proposed. Using this lipidomic approach, the effects of *N*-methyl-*N'*-nitro-*N*-nitrosoguanidine (MNNG) on sphingomyelin metabolism, a major class of sphingolipids, were evaluated. Sphingomyelin molecules were extracted from cells and analyzed by matrix-assisted laser desorption ionization-time of flight MS. It was found that MNNG induced profound changes in sphingomyelin metabolism, including the appearance of some new sphingomyelin species and the disappearance of some others, and the concentrations of several sphingomyelin species also changed. This was accompanied by the redistribution of acid sphingomyelinase (ASM), a key player in sphingomyelin metabolism. On the other hand, imipramine, an inhibitor of ASM, caused the accumulation of sphingomyelin. It also prevented some of the effects of MNNG, as well as the redistribution of ASM. Taken together, these data suggested that the lipidomic approach is highly effective for the systematic analysis of cellular lipids metabolism.

Key words lipidomics; mass spectrometry; ceramide; sphingomyelin; acid sphingomyelinase

The completion of the human genome project has led to a revolution in the world of biological science: the generation of "genomics". Following this event, "omics" in other disciplines also emerged, such as proteomics, metabonomics, toxicogenomics and pharmacogenomics [1,2]. All of these "omics", genomics and proteomics in particular, form the foundation for a new research field, systems biology. The goal of systems biology is to formulate a computational/mathematical model that describes the structure of the system and its response to individual perturbations through the monitoring of systematic changes of all cellular components (genes, proteins, or signaling pathways) in response to any type of perturbation (biological, genetic, or chemical) [3,4]. Therefore, it requires certain technical approaches which can define many cellular molecules at multiple levels; microarray for DNA analysis in genomics and 2-dimensional (2-D) gel electrophoresis combined with mass spectrometry (MS) for protein analysis in proteomics are just such methods.

It has been gradually recognized that studying DNA and protein alone does not engender a full understanding of a complex biological response, as other major cellular

Received: March 20, 2005 Accepted: May 23, 2005

This work was supported by the grants from the National Key Basic Research and Development Program (2002CB512901), National Hi-Tech Research and Development Program (2004AA649120), Natural Science Foundation of China (30300277 and 30471956), the Initiative Fund for Returned Oversea Chinese Scholars, Ministry of Education, China, and the Y.C. TANG Disciplinary Development Fund, Zhejiang University, National Institute of Health (NIH CA95393-01 and NIH P50 grant CA112970) and National Aeronautics and Space Administration (NASA NNA04CA75I), USA

[&] Present address: Department of Chemistry, Georgia State University, Atlanta, GA 30303, USA

[#] These authors contributed equally to this work

*Corresponding author: Tel/Fax, 86-571-87217149; E-mail, gastate@zju.edu.cn

DOI: 10.1111/j.1745-7270.2005.00073.x

constituents including lipids and carbohydrates are also involved in many physiological processes. Consequently, the lack of such information would hamper the construction of a computational model for systems biology. Recently, a new concept, "lipidomics", has been proposed [5,6]. Lipidomics is a comprehensive analysis of lipid molecules which, in combination with genomics and proteomics, is essential for the understanding of cellular physiology and pathology. Consequently, lipid biology has become a major research target of the postgenomic revolution and systems biology [7].

Lipids are crucial structural/functional components of cells. As structural material, they not only provide a physical barrier for cells, but also provide a platform (or lipid raft) for membrane protein-protein interaction. Even more importantly, many lipid species have distinct cellular functions. For example, diacylglycerol, ceramides, eicosanoids and lysolipids are all second messengers which participate in various cellular events such as growth, proliferation, differentiation and cell death [8]. Sphingolipids are a group of sphingoid-based lipids which are gaining increasing attention from researchers. They are the major components for lipid raft. Furthermore, sphingolipids and their metabolites are involved in many important signal transduction pathways which regulate such cellular processes as cell cycle arrest or apoptosis, proliferation and calcium homeostasis, as well as cancer development, multidrug resistance, and viral or bacterial infection processes [9]. Clearly, the importance of this group of lipids should not be underestimated.

Unfortunately, the study of lipids is far behind those of genes and proteins. One major obstacle is the lack of high-throughput technologies in lipid analysis. The traditional methods, such as isotope labeling, thin-layer chromatography and high performance liquid chromatography, could provide some useful information, but are far from adequate. Nevertheless, until the application of MS in sphingolipid study does a great amount of information is generated. Compared with traditional methods, MS analysis is more accurate, less labor-intensive and, most of all, can identify the molecular species of each class of lipids [10,11]. In our previous studies, using isotope labeling methods as well as matrix-assisted laser desorption ionization-time of flight (MALDI-TOF) MS, it has been shown that *N*-methyl-*N'*-nitro-*N*-nitrosoguanidine (MNNG), an alkylating agent which is a potent carcinogen, can affect ceramide metabolism [12,13]. Sphingomyelin is another important sphingolipid species closely related to ceramide metabolism, for example, sphingomyelin can be hydrolyzed to generate ceramide [9]. Therefore, it is quite reasonable to speculate that MNNG would also affect sphingomyelin metabolism.

In this research, we investigated the effects of MNNG on sphingomyelin metabolism. In addition, the cellular distribution of acid sphingomyelinase (ASM), a key enzyme in sphingomyelin metabolism, was also determined. As reported here, MNNG induced the generation/loss of some sphingomyelin species, as well as the increase/decrease of other sphingomyelin species.

Materials and Methods

Cell culture and reagents

Human amnion FL cells were cultured in Eagle's minimum essential medium (EMEM; Invitrogen, Carlsbad, USA) containing 10% fetal bovine serum, supplemented with 100 U/ml penicillin, 100 U/ml streptomycin and 0.03% *L*-glutamine in a humidified incubator at 37 °C with 5% CO_2. MNNG (Sigma, St. Louis, USA) was dissolved in dimethylsulfoxide (DMSO) as a 10 mM stock. Imipramine (Sigma) was also dissolved in DMSO as a 50 mM stock. For MNNG treatment, cells were treated with 10 μM of MNNG for 20 min. DMSO-treated or untreated cells were used as solvent control or blank control, respectively.

D-sphingosine, *N*-acetyl-*D*-sphingosine (C2-ceramide), *N*-hexanoyl-*D*-sphingosine (C6-ceramide), *N*-octanoyl-*D*-sphingosine (C8-ceramide), *D-threo*-ceramide C8, dihydrosphingosine, C2-dihydroceramide, C6-dihydroceramide, and C8-dihydroceramide were all purchased from Sigma; and each was dissolved following the manufacturer's instructions.

Immunofluorescent microscopy

The translocation of ASM was observed by immunofluorescent microscopy as described before [14]. Briefly, 1×10^5 FL cells were seeded into a 6-well culture plate with a glass cover slip in each well. After MNNG (10 μM) treatment for 20 min, cells were fixed and permeated with 100% ice-cold methanol for 5 min, followed by blocking in a blocking solution (Zymed Laboratories Inc., San Francisco, USA) for 2 h. The plate was washed with PBS three times and the polyclonal rabbit anti-ASM antibody (1:200; Santa Cruz Biotechnology, Santa Cruz, USA) was added and incubated for 90 min. Cy3-labeled goat anti-rabbit secondary antibody (1:200; Boster Biological Technology Limited, Wuhan, China) was then added to the plate and incubated for 1 h. These cells were

then washed and stained with 500 ng/ml FITC-cholera toxin B (Sigma) for 1 h. The cover slip was removed from the plate, mounted onto a glass slide, observed with an Olympus AX70 fluorescent microscope (Olympus, Tokyo, Japan), and analyzed using Image-Pro Plus software (MediaCybernetics, Silver Spring, USA). For imipramine treatment, cells were pre-incubated with 50 μM imipramine for 1 h before adding MNNG.

Sphingomyelin extraction and MALDI-TOF MS

Sphingomyelin was extracted as described before [12]. In short, approximately 4×10^7 cells were resolved in 500 μl chloroform:methanol (2:1, *V*/*V*). 1 ml H_2O was then added to each sample. The mixed samples were centrifuged at 4770 *g* for 15 min and the lower phase was dried by vacuum centrifugation in a centrifugal evaporator (Speed-Vac, Thermo Savant, Holbrook, USA). Then, 500 μl methanol containing 0.1 M NaOH was added into each tube at 55 °C for 1 h to decompose glycerophospholipids. After neutralization with 100 μl methanol containing 1 M HCl, 500 μl hexane and one drop of water were added to each sample. The mixture was then centrifuged again at 4770 *g* for 15 min and the lower phase was dried in a centrifugal evaporator after the upper phase was removed. The residue was mixed with 0.8 ml theoretical lower phase (chloroform:methanol:water, 86:14:1, *V*/*V*) and 0.2 ml theoretical upper phase (chloroform:methanol:water, 3:48:47, *V*/*V*) for the Folch partition, and centrifuged at 4770 *g* for 15 min. The lower phase was evaporated in a centrifugal evaporator after removing the upper phase to discard the salt. The residue crude sphingomyelin was stored at –70 °C.

For MALDI-TOF MS analysis, each sample was dissolved in 5 μl chloroform:methanol (2:1, *V*/*V*), followed by the addition of 5 μl matrix solution, ethylacetate containing 0.5 M 2,5-dihydroxyl-benzoic acid (2,5-DHB; Sigma) and 0.1% TFA, in a 0.5 ml Eppendorf tube. The tube was agitated vigorously on a vortex mixer then centrifuged in a microcentrifuge for 1 min. Then, 1 μl of mixture was directly added to the sample plate and rapidly dried under a warm stream of air in order to remove the organic solvent within seconds.

All samples were analyzed using a Voyager-DE STR MALDI-TOF mass spectrometer (ABI Applied Biosystem, Framingham, USA) with a 337 nm N_2 UV laser. The mass spectra of the samples were obtained in positive ion mode. Mass/charge (*m*/z) ratios were measured in the reflector/delayed extraction mode with an accelerating voltage of 20 kV, grid voltage of 67% and delay time of 100 ns. C2-dihydroceramide (MW 343.6) was used to calibrate the instrument. All sample lipid spectra were acquired using a low-mass gate at 400 Da. For each sample, 6 or 7 spectra were obtained; only when a peak appeared in at least 5 spectra with relatively stable intensity was it considered a candidate for analysis. All MS data were analyzed as described before [15,16].

Results

Establishment of MS data analysis protocol

In order to establish a working protocol for analyzing MS data for sphingolipids, up to 10 different sphingolipid species (natural or synthetic) were subjected to MS, and the major peaks from resulting mass spectra were calculated to deduce the possible chemical structures. The major peaks from two sphingolipids molecules, C8-ceramide and C8-dihydroceramide, are listed in **Table 1** and **Table 2**, respectively. 25 major peaks were generated by C8-ceramide during the ionization process, of which most were from the matrix 2,5-DHB. *m*/*z* 425 (425.6896) corresponded to the intact C8-ceramide. However, the relative intensity of this peak was only 14.17%; on the other hand, *m*/*z* 407 (407.7233) had a relative intensity of 100%. Based on calculation it was concluded that *m*/*z* 407 could stand for the fragment of C8-ceramide with an H_2O loss, suggesting that most C8-ceramide lost one molecule of water during ionization. Further chemical structural analysis gave two possible structures for this fragment [**Fig. 1(A)**]. The ionization process can even break the whole octal carbon sidechain away from a small portion (4.12%) of C8-ceramide, resulting in the formation of a *D*-sphingosine-like fragment, which corresponded to *m*/*z* 281 (281.3613). Two isotope peaks were also present for *m*/*z* 407 and one for 425 (**Table 1**). Similar analysis was also conducted for C8-dihydroceramide (**Table 2**), and the possible chemical structures for some fragments are depicted in **Fig. 1(B)**. Together, these processes formulated the basic protocol for sphingolipids MS data analysis.

MNNG induces dramatic changes in sphingomyelin metabolism

Previously we have shown that MNNG can induce changes in ceramide metabolism [12,13]. As sphingomyelin is closely associated with ceramide, we further examined the cellular sphingomyelin metabolism using MALDI-TOF MS. The major sphingomyelin peaks obtained from control, DMSO-treated, and MNNG-treated cells are listed in **Table 3**. It was found that while DMSO had only a

Table 1 MALDI-TOF MS analysis of C8-ceramide

Index	Centroid mass (*m*/*z*)	Charge (*z*)	Relative intensity (%)	Source
1	217.8414	0	6.23	Matrix
2	231.6644	1	4.05	?
3	263.8577	0	6.38	?
4	264.1504	1	11.88	?
5	265.1066	1	5.16	?
6	272.5887	0	11.08	Matrix
7	273.8165	0	15.67	Matrix
8	281.3613	0	4.12	$C_{18}H_{35}NO$
9	301.7986	0	4.32	Matrix
10	317.7744	0	3.60	Matrix
11	329.7930	0	2.40	Matrix
12	332.4761	1	34.47	?
13	333.4742	1	6.40	?
14	389.7198	1	4.76	Matrix
15	390.6614	1	5.62	Matrix
16	407.7233	1	100.00	$C_{26}H_{49}NO_2$
17	408.6847	1	51.31	Isotope peak
18	409.6962	1	15.02	Isotope peak
19	414.5155	1	5.28	Matrix
20	425.6896	1	14.17	C8-ceramide
21	426.6879	1	3.64	Isotope peak
22	436.4980	1	20.80	Matrix
23	437.4921	1	4.99	Matrix
24	447.6712	1	47.20	?
25	448.6611	1	16.08	?

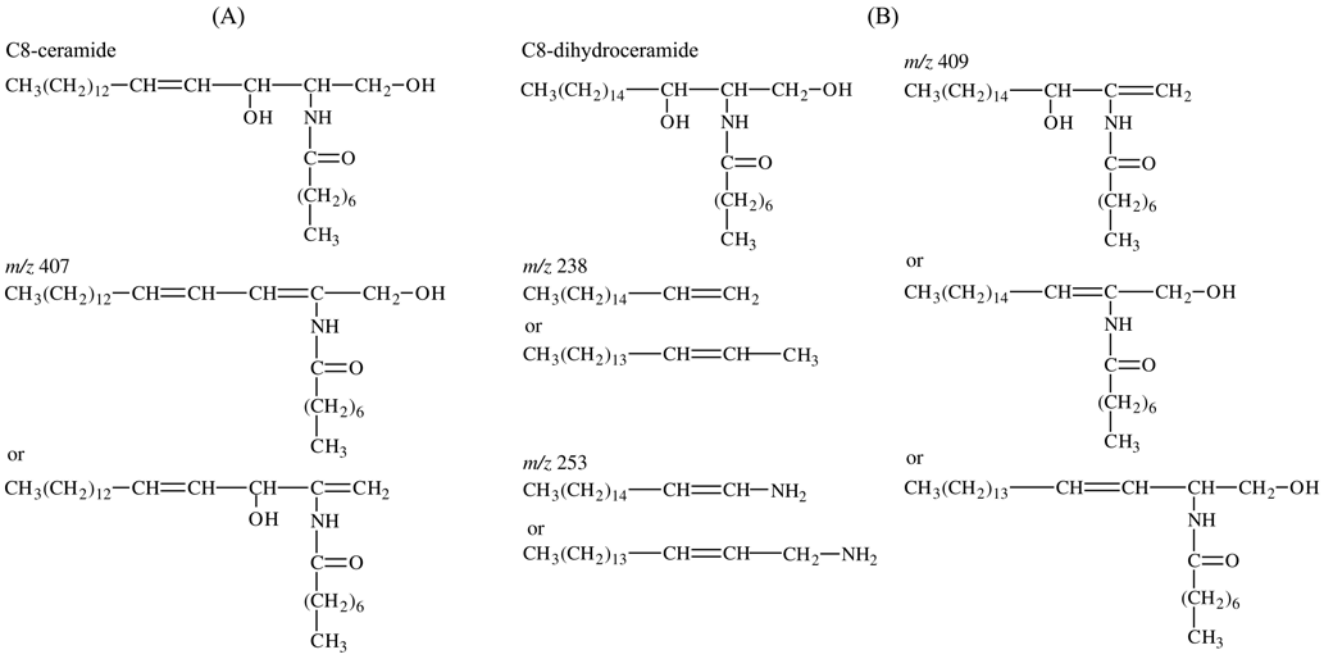

Fig. 1 Proposed chemical structures for fragmented C8-ceramide and C8-dihydroceramide

(A) *m*/*z* 407 from C8-ceramide. (B) *m*/*z* 238, 253 and 409 from C8-dihydroceramide.

Table 2 MALDI-TOF MS analysis of C8-dihydroceramide

Index	Centroid mass (*m*/*z*)	Charge (*z*)	Relative intensity (%)	Source
1	213.7746	1	6.98	Matrix
2	214.6713	1	6.28	Matrix
3	217.8310	1	4.43	Matrix
4	231.6403	1	8.96	?
5	232.6441	1	3.96	?
6	238.6498	0	5.47	$C_{17}H_{34}$
7	253.5839	1	2.96	$C_{17}H_{35}N$
8	254.5762	1	6.24	$C_{17}H_{35}N^{+}H$
9	272.5853	0	18.83	Matrix
10	273.8072	0	8.15	Matrix
11	301.7989	0	5.26	Matrix
12	332.4800	0	7.89	?
13	361.3734	0	8.03	Matrix
14	408.5005	1	11.66	?
15	409.7433	1	9.92	$C_{26}H_{51}NO_2$
16	410.6464	1	18.65	$C_{26}H_{51}NO_2{}^{+}H$ or isotope peak
17	411.6465	1	5.53	Isotope peak
18	427.7001	1	100.00	C8-dihydroceramide
19	428.6910	1	41.11	Isotope peak
20	429.7047	1	6.85	Isotope peak
21	433.7019	1	9.99	?
22	436.4803	1	26.59	Matrix
23	437.4847	1	7.64	Matrix
24	449.6603	1	59.32	?
25	450.6556	1	21.88	?

minor effect on sphingomyelin metabolism, there were significant differences between MNNG-treated and control samples for sphingomyelin. For example, *m*/*z* 778 was not present in control but appeared after MNNG treatment; whereas *m*/*z* 782 showed up in control but disappeared after MNNG treatment (**Table 3**). In addition, the concentrations of several sphingomyelin species, including *m*/*z* 770, 784, 805 and 814, were increased. The mass spectra data for some sphingomyelin species [**Fig. 2(A)**, *m*/*z* 782, 784, 805 and 814] and possible structures for some of the identified sphingomyelin species are also presented (**Table 4**).

MNNG induces the redistribution of ASM

ASM is responsible for hydrolyzing sphingomyelin to generate ceramide, and its translocation is usually associated with its activation [17–19]. Using immunofluorescent microscopy, the distribution of ASM and its relationship with lipid rafts were studied. ASM exhibited a diffused, even distribution in control cells [**Fig. 3(A)**] and DMSO solvent control (data not shown). However, MNNG treatment caused the "polarization" of ASM, which concentrated on one side of the cell [**Fig. 3(A)**]. In addition, ASM colocalized with lipid raft, which was labeled by cholera toxin B. This observation implied that ASM might be involved in the altered sphingomyelin metabolism.

Imipramine induces the accumulation of sphingomyelin and inhibits some of the effects of MNNG on sphingomyelin

Imipramine is known to inhibit ASM activity [20]. MNNG-induced changes in sphingomyelin may be a result of ASM activation, therefore cells were pre-incubated with imipramine followed with MNNG treatment and, after sphingomyelin extraction, the mass spectra were compared with those without imipramine. It was found that imipramine alone could cause the accumulation of several sphingomyelin species, indicating that it inhibited the hydrolysis of sphingomyelin (**Table 3**). Furthermore, it diminished some effects of MNNG on sphingomyelin. For example,

Table 3 The effects of MNNG on sphingomyelin metabolism

m/*z*	Imipramine (–)			Imipramine (+)		
	Blank	DMSO	MNNG	Blank	DMSO	MNNG
725 (t18C16h:0) [M]	++	++	++	++	++	+
748 (d18C20:0) $[M+H]^+$ (t18C16h:0) $[M+Na]^+$				++	+	+
770 (d18C20:0) $[M+Na]^+$ (t18C19:0) $[M+H+H_2O]^+$	+	+	++	+	+	+
778 (d18C21:1) $[M+H+H_2O]^+$ (t18C21:1) $[M+H]^+$ (d18C21h:0) $[M+H]^+$			++			+
782 (d18C21:1) $[M+Na]^+$ (t18C20:1) $[M+H+H_2O]^+$ (d18C20h:0) $[M+H+H_2O]^+$ (t18C20h:0) $[M+H]^+$	+	+		+++	++	++
784 (d18C21:0) $[M+Na]^+$ (t18C20:0) $[M+H+H_2O]^+$	+		++	++	++	+
805 (t18C23:1) [M] (d18C23h:0) [M]	+	+	++		+	++
814 (t18C22:1) $[M+Na]^+$ (d18C22h:0) $[M+Na]^+$ (t18C21h:0) $[M+H+H_2O]^+$	+	+	++	++	+	++

the increases of *m*/*z* 770 and 784 by MNNG treatment were reversed by imipramine pre-incubation, and the disappeared *m*/*z* 782 was restored [**Table 3**, **Fig. 2(B)**]. Furthermore, imipramine also prevented the polarization of ASM induced by MNNG, implying the inactivation of ASM [**Fig. 3(B)**].

Discussion

Many sphingolipid molecules, such as ceramide, sphingosine and sphingosine-1-phosphate, are increasingly recognized as important modulators of many cellular processes. For example, ceramide has been shown to function as a second messenger for Fas, tumor necrosis factor, interleukin (IL-1) and other cytokines, as well as many other extracellular stimuli, usually with the result of either cell cycle arrest or apoptosis [9,13,21,22]. However, unlike nucleotides and proteins, lipids and sphingolipids, have long been a group of molecules that are difficult to study. Sphingolipids were named after the famous Egyptian statue "Sphinx" for their mystical properties. The bottleneck in research was due to the lack of suitable technologies for analyzing the vast number of lipid species, even less the high-throughput technology for systems biology.

The breakthrough came after the application of MS to lipid study, in which many molecules from the lipidome could be directly characterized and quantitated [8,10,11]. Using this method, we have shown that MNNG can affect the metabolism of a major sphingolipid species, ceramide [12]. This change of metabolism is associated with some of the cellular effects of MNNG, such as membrane receptor clustering [12]. In this study, we further evaluated

Table 4 Proposed structures for some identified sphingomyelin species

m/z	Proposed structure
770 (d18C20:0) $[M+Na]^+$	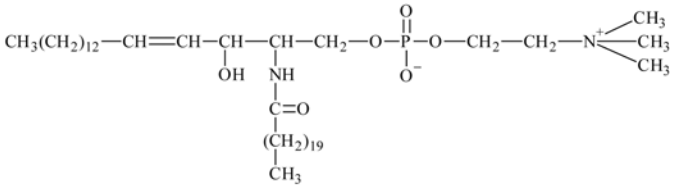
(t18C19:0) $[M+H+H_2O]^+$	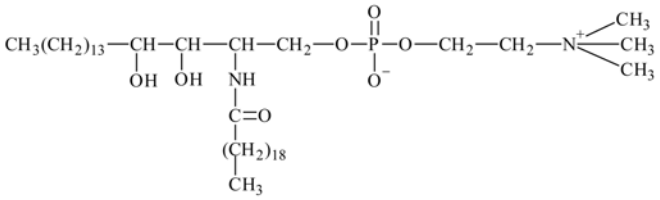
782 (d18C21:1) $[M+Na]^+$	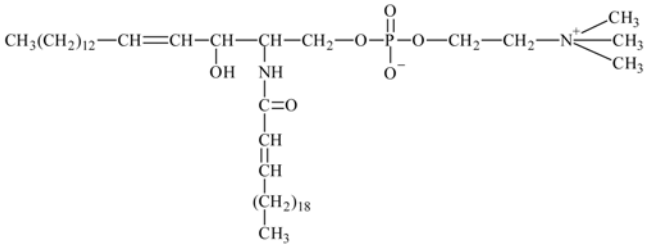
(t18C20:1) $[M+H+H_2O]^+$	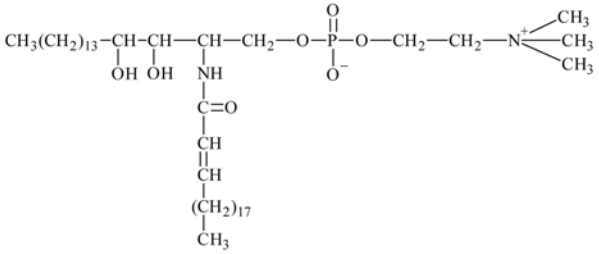
(d18C20h:0) $[M+H+H_2O]^+$	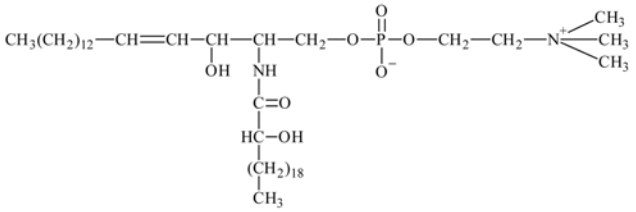
(t18C20h:0) $[M+H]^+$	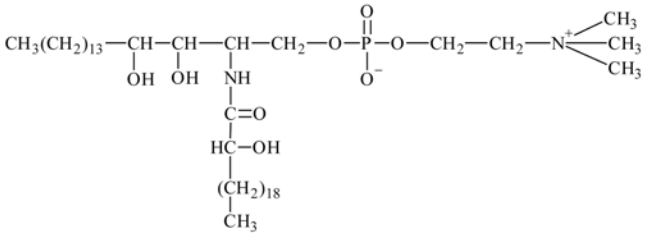

the metabolism of sphingomyelin, which can be hydrolyzed by ASM to generate ceramide [9]. It was found that, similar to ceramide, sphingomyelin metabolism was also affected by MNNG treatment (**Table 3**), indicating that MNNG may have a global effect on sphingolipids metabolism.

More importantly, using this MS approach, the different sphingomyelin species could be identified, and the changes for each species measured. For instance, eight distinct *m/z* ratios were identified, with each *m/z* ratio represent-

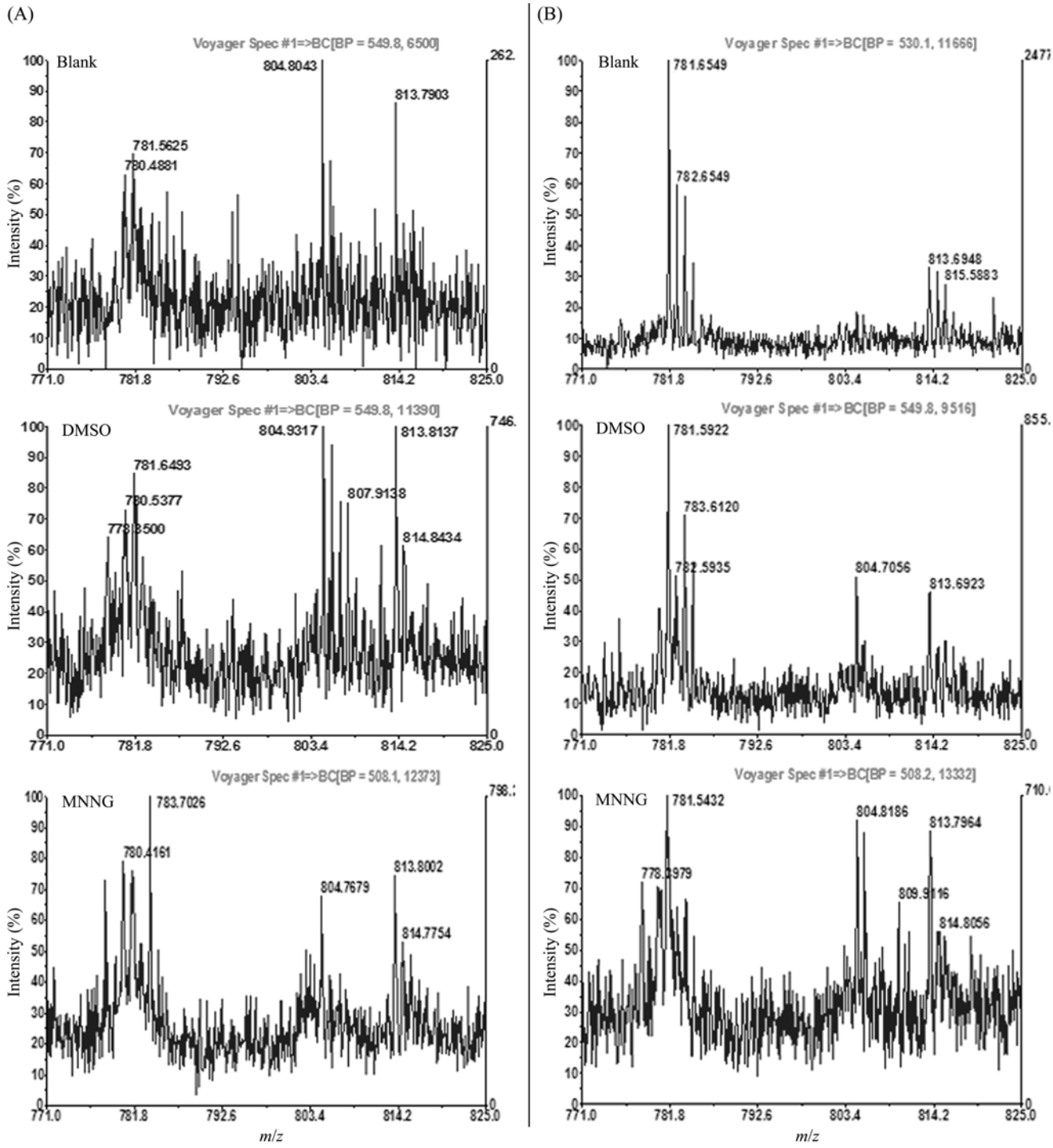

Fig. 2 MNNG induces changes in sphingolipids metabolism

After 30 min of treatment, lipids were extracted and subjected to mass spectrometry analysis as described in "Materials and Methods". (A) Representative mass spectrometry data after MNNG treatment. *m*/*z* range was 770–826. (B) Representative mass spectrometry data with imipramine pre-incubation followed by MNNG treatment. *m*/*z* range was 770–826.

ing one or more possible molecular structures (**Table 3**). The differences in sidechain length, as well as the number of unsaturated bonds, may influence the function of a specific lipid molecule. Therefore, this type of analysis

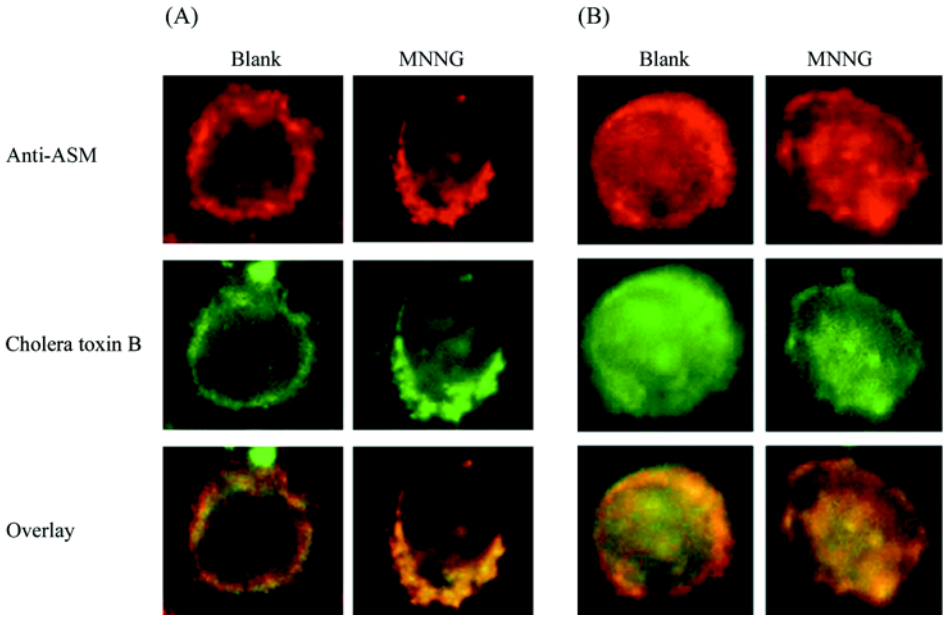

Fig. 3 MNNG induces the redistribution of ASM

(A) After MNNG treatment for 30 min, cells were stained with anti-ASM antibody and Cy3-labeled secondary antibody. After washing, cells were further stained with FITC-cholera toxin B (CtxB) for 1 h. The images were captured with an Olympus AX70 fluorescent microscope and analyzed using Image-Pro Plus software. (B) Cells were pre-incubated with imipramine for 1 h before MNNG treatment; the distribution of ASM was then observed as described above. Magnification, 400×.

provides invaluable information that cannot be obtained using traditional methods.

The applicability of this technique was further validated by the imipramine experiment. As an inhibitor for ASM, it was expected that imipramine would inhibit the hydrolysis of sphingomyelin, thus increasing the cellular content of sphingomyelin. Indeed it was found that imipramine treatment caused the accumulation of several sphingomyelin species, particularly *m*/*z* 748 and 782 [**Table 3**, **Fig. 2(B)**]. In addition, imipramine pre-incubation interfered with the effect of MNNG on sphingomyelin, indicating that MNNG probably elicited its effect through the action of ASM. This was also supported by the immunfluorescent microscopy data, as MNNG treatment triggered the relocation of ASM, while imipramine prevented it (**Fig. 3**).

Some problems do exist for the MS method. For example, except for a few *m*/*z* ratios, exact chemical structures could not be deduced precisely; instead, several possibilities were formulated. Furthermore, when standard sphingolipids were subjected to MALDI-TOF analysis, several fragments were generated for each standard (for example, *m*/*z* 407 and 281 for C8-ceramide). It would be difficult to tell if these fragments were the original forms presented in the sample or just fragments generated from other molecules during the ionization process. The presence of matrix peaks complicates the analysis even further. Finally, the reproducibility of mass spectra should be carefully handled. Mass spectrometry is a very sensitive method and efforts should be taken to minimize the variations which might affect the analyses.

Compared with MALDI-TOF, liquid chromatography-electrospray ionization MS (LC-ESI MS) may prove to be a better solution. First, there is no need for matrices in the analysis. Secondly, its “soft” ionization process, generally, would not fragment the samples. Therefore, LC-ESI MS has far less “noise” than MALDI-TOF MS. Nevertheless, there is the possibility that two molecules have distinct structures but the same molecular weight. To solve this problem, Han and Cheng developed a 2-D ESI MS/MS method [10]. Through lipid class-selective intrasource ionization and subsequent analysis of 2-D cross-peak intensities, the chemical identity and mass composition of individual molecular species of most lipid classes can be determined [10].

In summary, the data presented here demonstrated that MALDI-TOF MS is a powerful tool in lipid research. Together with the 2-D ESI MS/MS method, these techniques provide a strong foundation for the automated analysis of lipid mass spectra data, which will help to push

the study of systems biology to a new level.

Acknowledgements

The authors gratefully thank Dr. T. TAKETOMI for providing detailed instructions for analyzing the MALDI-TOF mass spectrometry data, and Dr. X. HAN for the helpful discussion regarding lipidomics.

References

1 Pognan F. Genomics, proteomics and metabonomics in toxicology: Hopefully not 'fashionomics'. Pharmacogenomics 2004, 5: 879–893
2 Kramer R, Cohen D. Functional genomics to new drug targets. Nat Rev Drug Discov 2004, 3: 965–972
3 Aggarwal K, Lee KH. Functional genomics and proteomics as a foundation for systems biology. Brief Funct Genomic Proteomic 2003, 2: 175–184
4 Kell DB. Metabolomics and systems biology: Making sense of the soup. Curr Opin Microbiol 2004, 7: 296–307
5 Han X, Gross RW. Global analyses of cellular lipidomes directly from crude extracts of biological samples by ESI mass spectrometry: A bridge to lipidomics. J Lipid Res 2003, 44: 1071–1079
6 Lagarde M, Geloen A, Record M, Vance D, Spener F. Lipidomics is emerging. Biochim Biophys Acta 2003, 1634: 61
7 Fahy E, Subramaniam S, Brown HA, Glass CK, Merrill AH Jr, Murphy RC, Raetz CR *et al*. A comprehensive classification system for lipids. J Lipid Res 2005, 46: 839–862
8 Han X, Yang J, Cheng H, Ye H, Gross RW. Toward fingerprinting cellular lipidomes directly from biological samples by two-dimensional electrospray ionization mass spectrometry. Anal Biochem 2004, 330: 317–331
9 Yang J, Yu Y, Sun S, Duerksen-Hughes PJ. Ceramide and other sphingolipids in cellular responses. Cell Biochem Biophys 2004, 40: 323–350
10 Han X, Cheng H. Characterization and direct quantitation of cerebroside molecular species from lipid extracts by shotgun lipidomics. J Lipid Res 2005, 46: 163–175
11 Han X, Gross RW. Shotgun lipidomics: Electrospray ionization mass spectrometric analysis and quantitation of cellular lipidomes directly from crude extracts of biological samples. Mass Spectrom Rev 2005, 24: 367–412
12 Huang Y, Yang J, Shen J, Chen F, Yu Y. Sphingolipids are involved in N-methyl-N′-nitro-N-nitrosoguanidine-induced epidermal growth factor receptor clustering. Biochem Biophys Res Commun 2005, 330: 430–438
13 Yang J, Duerksen-Hughes PJ. Activation of a p53-independent, sphingolipid-mediated cytolytic pathway in p53-negative mouse fibroblast cells treated with N-methyl-N-nitro-N-nitrosoguanidine. J Biol Chem 2001, 276: 27129–27135
14 Gao Z, Yang J, Huang Y, Yu Y. N-methyl-N′-nitro-N-nitrosoguanidine interferes with the epidermal growth factor receptor-mediated signaling pathway. Mutat Res 2005, 570: 175–184
15 Fujiwaki T, Yamaguchi S, Tasaka M, Sakura N, Taketomi T. Application of delayed extraction-matrix-assisted laser desorption ionization time-of-flight mass spectrometry for analysis of sphingolipids in pericardial fluid, peritoneal fluid and serum from Gaucher disease patients. J Chromatogr B Analyt Technol Biomed Life Sci 2002, 776: 115–123
16 Fujiwaki T, Yamaguchi S, Sukegawa K, Taketomi T. Application of delayed extraction matrix-assisted laser desorption ionization time-of-flight mass spectrometry for analysis of sphingolipids in cultured skin fibroblasts from sphingolipidosis patients. Brain Dev 2002, 24: 170–173
17 Grassme H, Cremesti A, Kolesnick R, Gulbins E. Ceramide-mediated clustering is required for CD95-DISC formation. Oncogene 2003, 22: 5457–5470
18 Gulbins E, Grassme H. Ceramide and cell death receptor clustering. Biochim Biophys Acta 2002, 1585: 139–145
19 Gulbins E. Regulation of death receptor signaling and apoptosis by ceramide. Pharmacol Res 2003, 47: 393–399
20 Lacour S, Hammann A, Grazide S, Lagadic-Gossmann D, Athias A, Sergent O, Laurent G *et al*. Cisplatin-induced CD95 redistribution into membrane lipid rafts of HT29 human colon cancer cells. Cancer Res 2004, 64: 3593–3598
21 Pru JK, Hendry IR, Davis JS, Rueda BR. Soluble Fas ligand activates the sphingomyelin pathway and induces apoptosis in luteal steroidogenic cells independently of stress-activated p38(MAPK). Endocrinology 2002, 143: 4350–4357
22 Luberto C, Hassler DF, Signorelli P, Okamoto Y, Sawai H, Boros E, Hazen-Martin DJ *et al*. Inhibition of tumor necrosis factor-induced cell death in MCF7 by a novel inhibitor of neutral sphingomyelinase. J Biol Chem 2002, 277: 41128–41139

Edited by
Shu-Sen LIU